Pitch-Controlled Landing for Airborne Ground Vehicles

Manasa Sathyan
MSE ROBO
msathyan@seas.upenn.edu

Mengti Sun
MSE ROBO
mengti@seas.upenn.edu

Nicholas Gurnard
MSE ROBO
ngurnard@seas.upenn.edu

Rithwik Udayagiri
MSE ROBO
rithwiku@seas.upenn.edu

***Abstract*—In this project, the aim is to attain optimal landing for an airborne autonomous ground vehicle. This is achieved by controlling the pitch of the vehicle by spinning the wheels mid-air and utilizing a PID controller for precision control. The PID controller tracks the pitch angle of the vehicle and commands an appropriate linear speed to ensure that the vehicle lands at the desired angle. Due to the absence of accurate model dynamics of the airborne vehicle, a simulator was first developed to evaluate the performance of the PID controller before tuning it on actual hardware. Repeatable, optimal landing was achieved on subsequent experimentation on the real car over multiple surfaces with different friction coefficients.**

***Index Terms*—pitch control, PID control, autonomous racing, off-road racing**

I. Introduction

Many of the autonomous racing solutions today depend on a 2D Birds-Eye-View (BEV) and largely ignore the vertical axis. For many planning problems, such as overtaking or obstacle avoidance on the ground, this is usually enough. However, not all applications can accurately ignore the vertical dimension. A popular application is off-road racing which involves maneuvering through uneven terrain that often contain elevation changes. When landing on a ramp or hill, a precise landing angle is critical for a successful and fast race outcome. We develop a robust control system that can autonomously adjust the pitch of the car mid-air, ensuring an optimal landing angle.

The aim of the project is to maintain optimal racing conditions despite becoming airborne. Namely, ensuring that the vehicle lands optimally and continues along a race line as fast as possible despite having no control from contact forces mid-air. In order to land optimally after becoming airborne, one can spin the wheels in the air to change the moment of inertia and induce pitch on the vehicle. Given that the desired landing angle is given, one can control the pitch of the vehicle to ensure optimal landing. An illustration of the problem can be seen in Fig 1.

In order to tackle the problem without having to build an accurate dynamics model, the project can be accomplished with a PID controller. A PID controller, however, is a single-input-single-output controller (SISO), so the full vehicle state cannot be taken into account while deciding a control action. Therefore, a simulator for the dynamic model was built in addition to creating and tuning a PID controller on real hardware.

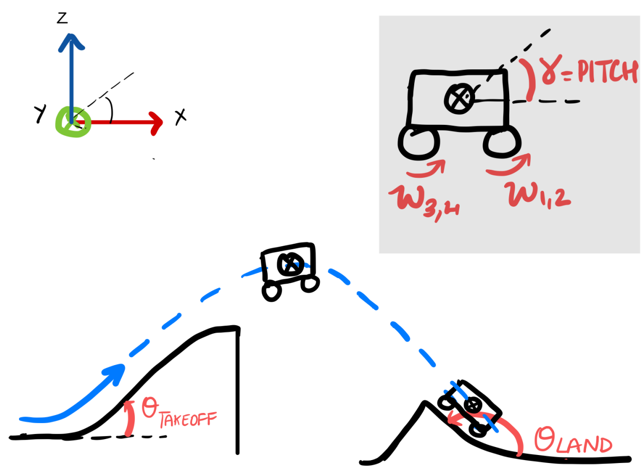

Fig. 1. Problem Sketch

For experimentation on the actual vehicle, setup details are discussed in section IV. Extensive testing and documentation on our findings are in section V. It was found that the approach taken is viable with some caveats.

Contributions: All team members contributed to the experimentation of the project on the physical hardware in roughly equal amounts. Simulation ideation was discussed with the team and implemented in code largely by Mengti. The controller and the ROS2 code was written largely by Nick and Rithwik. Early stage vehicle testing was spearheaded by Nick and Manasa. Later stage vehicle testing was taken on by Rithwik, Mengti, and Manasa. Data analysis, data collection, and report contributions were contributed to by the whole team equally. In summary, every team member had equal roles in the project.

II. Related Work

Works such as [3], [4], [5], [6], [7], and [8] have worked to plan trajectories over the 3rd vertical dimension to minimize energy consumption, speed, and comfort over an outdoor terrain. However, the event where there is an opportunity for the vehicle to go airborne to minimize control effort or lap time in a racing context has been largely unexplored.

Videos such as the ones in [9] [10] demonstrate how a vehicle can control the pitch of the vehicle in the air and served as our primary motivation for our project. The video demonstrates the pitch of the RC Cars being changed mid-air that enables the cars to land safely and optimally. For the model, the dynamics of a car taking off a ramp with pitch control have been well-modeled in video games like Hill Climb Racing [1] [2]. Additionally, [11] was a helpful resource to model the dynamics of our problem.

III. Methodology

A. Model Dynamics

The model for the change in pitch of the car was based on the wheel's angular velocities, following the Law of Conservation of Angular Momentum as discussed in [11].

To simplify the model, the front and rear wheels and the axles are estimated to be a solid cylinder. The car was approximated as a cuboid to calculate the moment of inertia. Angular momentum of each of the bodies is described by spin angular momentum, which is angular momentum around the center of mass. The angular momentum is transferred between the two bodies in a single axis.

Wheel as solid cylinder:

$$I_w = \frac{1}{2} m_w r_w^2$$
$$\omega_w = \frac{v_w}{r_w}$$

Axle as solid cylinder:

$$I_a = \frac{1}{2} m_a r_a^2$$
$$\omega_w = \frac{v_a}{r_a}$$

Car as solid cuboid:

$$I_c = \frac{m_c(l^2 + h^2)}{12}$$

Conservation of Angular Momentum:

$$I_c \omega_c = 4(I_w \omega_w) + 2(I_a \omega_a)$$
$$\omega_c = \frac{v_c}{r_w} \frac{12 \times 2(m_w r_w^2 + 0.5 m_a r_a^2)}{m_c(l^2 + h^2)} \quad (1)$$

Symbol	Entity	Unit
m_w	Mass of Wheel	kg
r_w	Radius of Wheel	m
I_w	Moment of Inertia of Wheel	kgm^2
ω_w	Angular Velocity of Wheel	rad/s
m_a	Mass of Axle	kg
r_a	Radius of Axle	m
ω_a	Angular Velocity of Axle	rad/s
I_a	Moment of Inertia of Axle of Wheel	kgm^2
m_c	Mass of Car	kg
l	Length of car	m
h	Height of car	m
v_c	Linear Velocity of Car	m/s
ω_c	Angular Velocity of Car	rad/s
I_c	Moment of Inertia of Car	kgm^2

TABLE I
SYMBOLS USED IN EQUATION 1

B. Simulator

In simulation, the trajectory of the car is represented as a projectile motion:

$$x_t = v_0 t \cos(\theta) \quad (2)$$
$$y_t = v_0 t \sin(\theta) - \frac{1}{2} g t^2 \quad (3)$$

where v_0 is the take-off velocity, θ the initial angle, g the acceleration due to gravity which is $9.8 m/s^2$, and x_t, y_t the position of current timestamp. Since IMU data isn't readily available in simulation, the pitch of the car, ψ_t, was calculated based on the previously commanded velocity and the time difference between them. The linear velocity of the wheels is mapped to the angular velocity of the car based on the dynamical model as stated in 1. Specifically, with angular momentum of the wheels and axles and the moment of inertia of the car body, we calculate the angular velocity of the car at timestamp t, ω_t. The pitch angle for the current timestamp ψ_t is obtained by:

$$\psi_t = \psi_{t-1} + \omega_{t-1} dt \quad (4)$$

At each timestamp, the error between the current pitch angle and the landing ramp angle (desired pitch angle) was found. This error is used with the PID controller to calculate the linear velocity of the current timestamp. The entire 2D trajectory was simulated with multiple initial angles, take-off velocity and PID values for feasibility analysis. A comparision of the controlled and uncontrolled trajectory is shown in Fig 2.

C. State Estimation

A UKF was implemented, but since the model was not highly accurate, the UKF state estimation was discarded and the state estimate relied on raw IMU values to decrease compute overhead. Since, PID gives feedback, it was robust to no state estimation.

IV. Experimental Setup

A. Initial Tethered Pitch Control

In order to study the pitch rotation of the F1TENTH car, the vehicle was suspended using a sturdy wire along its center of mass, as depicted in the Fig 3. Next, maximum throttle was applied in both forward and backward directions via the joystick controller. Observations indicated that the car pitched upwards when the wheels moved forward and pitched downwards when the wheels moved backwards, as expected.

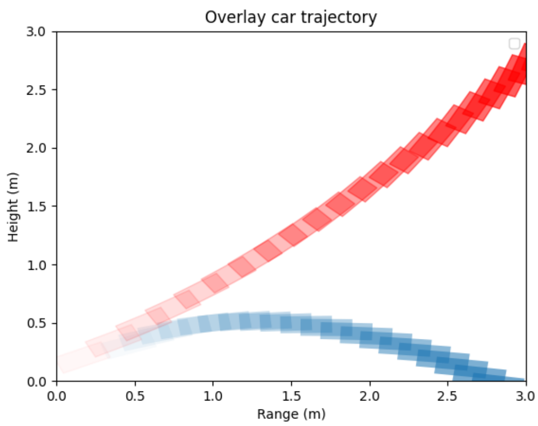

Fig. 2. Overlay trajectory with initial angle 22 degrees and take-off velocity $6.5m/s$. The red patches simulate trajectory with no PID and velocity $3.0m/s$ in the air. The blue patches simulate trajectory with PID control, $kp = 6.0, kd = 1e-5, ki = 1e-5$.

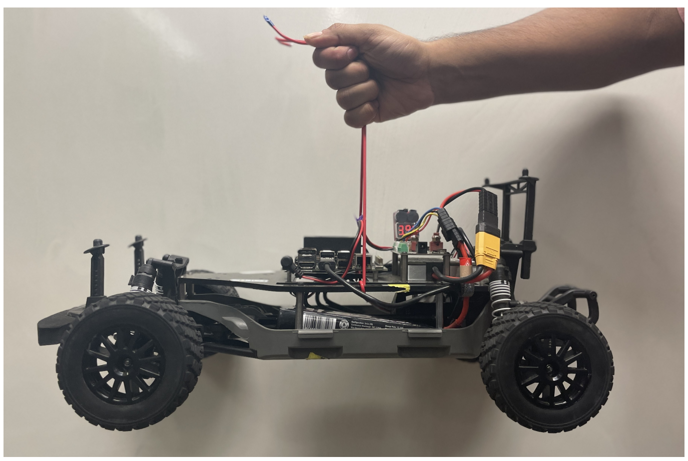

Fig. 3. Initial Tethered Pitch Control

B. Car Setup

The nature of the project required the F1TENTH car to be airborne at high speeds. Before conducting any tests, the LiDAR was taken out of the car as a safety precaution, as depicted in Figure 3. It was deemed unnecessary for the project's objectives. Further, the body of the vehicle was covered with a plastic body as seen in Fig 4 and was secured using body clips for extra protection of the computer and electronics.

C. Joystick Mapping to indicate Takeoff and Landing

A button was mapped to the controller that marked when to activate an autonomous ramp up pattern that accelerated up to the desired take-off speed of $6.5m/s$. Additionally, there was a separate button used for pitch control and another unique button pressed to indicate when landing occurred. This is necessary in order to line up cross-experiments and analyze trends accurately as shown in Fig 5

Fig. 4. Protected Car

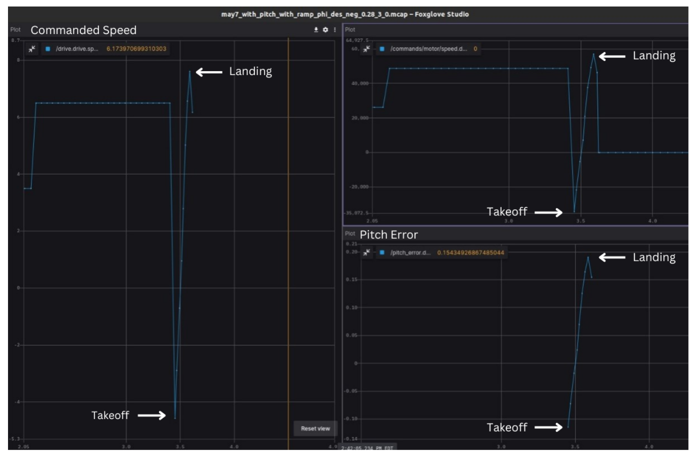

Fig. 5. Indication of Airborne Pitch Control

D. Outdoor Experimentation Setup

Initially, the experiments were set up outdoors as shown in Fig 6 to simulate a realistic environment. A patch of lawn was chosen instead of hard ground to test the airborne car for an added layer of protection. However, due to unpredictable weather conditions, the team had to eventually shift experiments to an indoor setting. Moreover, the risk of dew on the lawn splashing onto the Jetson presented a potential hazard.

E. Indoor Experimentation Setup

The final experimental setup consisted of the F1TENTH car, acrylic takeoff and landing ramps, and compliant plastic hollow duct tubes for cushioning as seen in Fig 7. The takeoff ramp was mounted at a fixed angle of $\theta = 22°$. This angle proved to be the best choice in the experimentation to achieve significant air time at the car's speed. The landing ramp was then setup at the desired landing angle ψ_{des} and at a distance d away from the takeoff ramp. This horizontal distance traveled

Fig. 6. Outdoor Experiment Setup

by the car can be calculated using the projectile motion as seen in equations (2) and (3),

$$d = (v_0^2 sin(2\theta))/g \tag{5}$$

where v_0 is the initial velocity, θ the initial ramp angle, and g the acceleration due to gravity which is approximately 9.81 m/s^2.

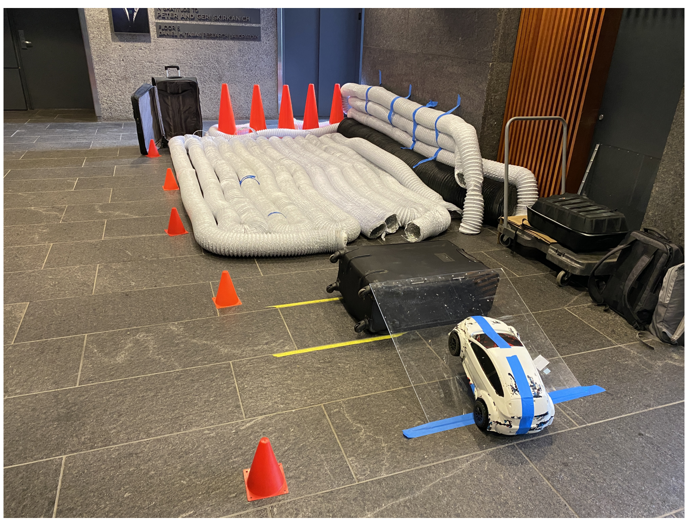

Fig. 7. Indoor Experiment Setup

V. Experiments and Results

A. Simulator Setup and Results

In order to accurately simulate the vehicle pitch, physical parameters in table I were measured on the hardware. These are shown in table II and their accuracy showed a similarity between Simulation and Real results.

With the same environmental parameters as in Fig 2, the simulation result is shown in Fig 8. The pitch angle converges to ψ_{des} with a pitch error on the scale of 1e-2. The pitch error is minimized during landing and the velocity profile is smooth.

Symbol	Value
m_w	0.1802kg
r_w	0.04826m
m_a	0.1kg
r_a	0.01115m
m_c	2.4192kg
l	0.3303m
h	0.145m

TABLE II
Real Car values used in Simulator

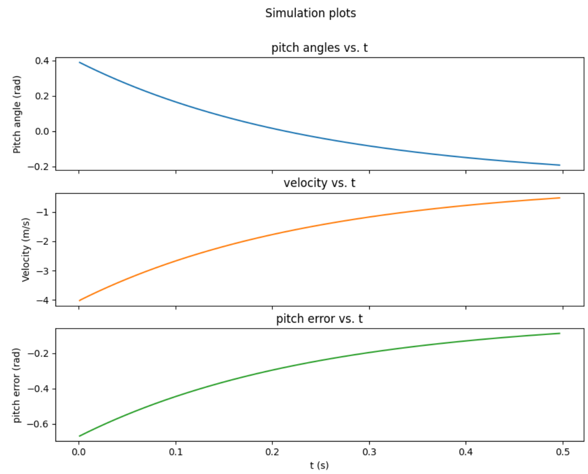

Fig. 8. Plot of pitch angles, velocity and pitch errors of simulated data.

B. Actual Hardware Experiments and Results

In all experiments, the vehicle was sent at a speed of $6.5m/s$ off of the ramp. For experiments with pitch control, once the rear wheels of the vehicle took off from the ramp, pitch control was activated until the vehicle landed again. For the experiment without pitch control, the vehicle was commanded zero driving speed such that the wheels did not spin at all once airborne.

1) Teleop Only - No pitch control: It is necessary to collect data as a baseline to evaluate whether or not the implemented strategies work as intended. The vehicle was controlled via teleop (joystick controller) and sent off of the launching platform without any pitch control efforts in the air. Data on the pitch, speed, orientation, etc. over time from start of time of flight to landing was recorded. It was found that the vehicle consistently would land nose down on the landing pad, and would often tumble into an uncontrolled crash. This was expected since the vehicle is all wheel drive, and this once the front wheels are airborne, the back wheels are still accelerating up the ramp sending the nose downward.

2) Pitch control - Without Landing Ramp: The vehicle pitch control was initially implemented on a crash pad with a commanded desired pitch angle of 0°. Simulator parameters were initially used, and kp, kd were further tuned to minimize the sim-to-real gap. It was observed that the vehicle would not nose dive as harshly as before and regularly land in a controlled near $0°$ fashion, as shown in Fig 9, there was overshooting with pitch errors which was 0.26 radian during landing. This result was expected due to projectile motion dynamics and the slow response time of the motors making the vehicle less responsive than desired.

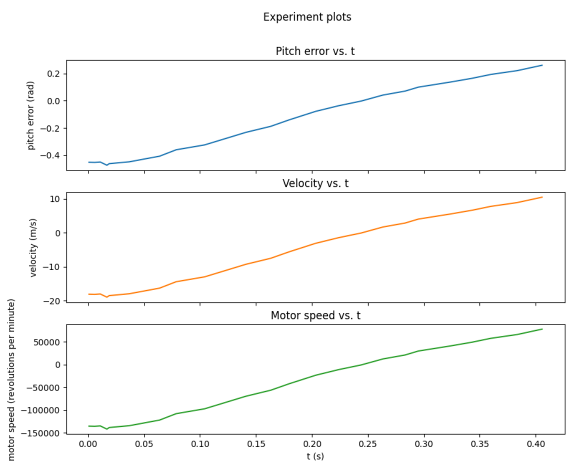

Fig. 9. Plot of pitch angles, velocity and pitch errors of experiment without landing ramp. Experiment parameters include initial angle 23 degrees, landing angle 0 degrees and take-off velocity $6.5m/s$, $kp = 30.0, ki = 1e-5, ki = 1e-5$.

3) Pitch control - With Landing Ramp: The vehicle pitch control was then experimented on ramps separated by a certain distance calculated in equation 5 depending on the take-off velocity. As shown in Fig 10, pitch errors converges to 0.047 radians during landing. The velocity profile is smooth and the motor is responsive.

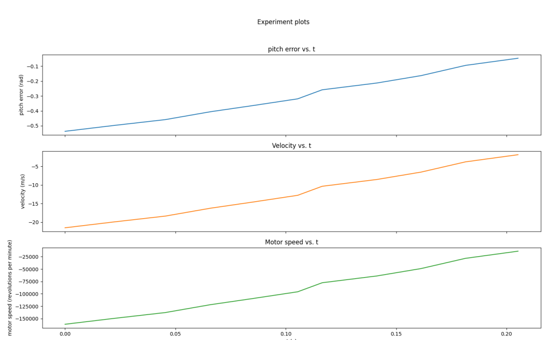

Fig. 10. Plot of pitch angles, velocity and pitch errors of experiment with landing ramp. Experimental parameters include initial angle 23 degrees, landing angle -20 degrees, distance between ramps $2.34m$, take-off velocity $6.5m/s$, $kp = 40.0, ki = 1e-5, kd = 1e-5$.

VI. Conclusion

It was found that the setup on the hardware was feasible and successful, however had room for improvement. The vehicle was able to successfully achieve the desired pitch angle across multiple tests, however was not close to 100% repeatable. It was found that the vehicle achieved the desired landing angle approximately 85% of the time, with the failed tests often occurring due to operator error or slow response on the hardware. It is possible that the software stack itself was slow, however highly unlikely given that the controller was a PID controller that did not require heavy compute from optimization or localization. Additionally, the air time of the vehicle was limited, as seen throughout the plots in the experiments, which made it difficult to fully visualize and realize how robust the PID controller was. It was enough and was successful on the hardware for this robot, however was not tested across multiple lengths of airtime. Overall, the project was successful in its scope.

VII. Future Work

Building a more accurate dynamics model would allow the team to explore vastly more control opportunities such as MPC, LQR, etc. With a more complex control scheme, it would be fitting to add complexity by using a vision system to gather a more accurate state estimate or building a map. With a map in 3D, the vehicle can plan in 3D such that it knows when to go for a big jump or slow down to keep traction and control authority through contact. Additionally, a map would inform the vehicle of when it is airborne and what the landing angles should be.

Additionally, the state estimate of the vehicle was obtained from the VESC IMU onboard. Inherently there was some noise in the system, however it sufficed for the purpose of this project. In the future when the control becomes more complex or responsive, it would be appropriate to also implement a more accurate state estimator with an EKF or UKF.

Finally, the F1TENTH Traxxas body have motors that have slow response time, compromising the responsiveness of the controllers in the air. In order to command more authority in the air, it would be advantageous to get motors with a much faster ramp up and ramp down speed.

References

[1] Pierluigi, A., Valerio, C. (2013). Design and Development of Contractive Suspension in Hill-Climb Races. In: Proceedings of the FISITA 2012 World Automotive Congress. Lecture Notes in Electrical Engineering, vol 195. Springer, Berlin, Heidelberg. https://doi.org/10.1007/978-3-642-33835-9-49

[2] Zhang, Xin. "Aerodynamic model of a hill climb racing car." Bernoulli Aerodynamics International (2007).

[3] Meng, Xiangyun, et al. "TerrainNet: Visual Modeling of Complex Terrain for High-speed, Off-road Navigation." arXiv preprint arXiv:2303.15771 (2023).

[4] K. Chu, M. Lee and M. Sunwoo, "Local Path Planning for Off-Road Autonomous Driving With Avoidance of Static Obstacles," in IEEE Transactions on Intelligent Transportation Systems, vol. 13, no. 4, pp. 1599-1616, Dec. 2012, doi: 10.1109/TITS.2012.2198214.

[5] Y. Ji, L. Ni, C. Zhao, C. Lei, Y. Du and W. Wang, "TriPField: A 3D Potential Field Model and Its Applications to Local Path Planning of Autonomous Vehicles," in IEEE Transactions on Intelligent Transportation Systems, vol. 24, no. 3, pp. 3541-3554, March 2023, doi: 10.1109/TITS.2022.3231259.

[6] Tian, Hongqing, et al. "Driving risk-aversive motion planning in off-road environment." Expert Systems with Applications 216 (2023): 119426.
[7] Chu, K., Kim, J., Jo, K. et al. Real-time path planning of autonomous vehicles for unstructured road navigation. Int.J Automot. Technol. 16, 653–668 (2015). https://doi.org/10.1007/s12239-015-0067-5
[8] Williams, Grady, et al. "Autonomous racing with autorally vehicles and differential games." arXiv preprint arXiv:1707.04540 (2017).
[9] Video demonstration of controlling vehicle pitch. https://www.instagram.com/reel/CrrzX0cp8nw/?igshid=YmMyMTA2M2Y=
[10] Off-Road RC Car Championship. https://www.youtube.com/watch?v=fn02DjC0gok&t=27s
[11] Pitch Control https://physics.stackexchange.com/questions/734513/could-pressing-the-brakes-on-a-car-in-mid-air-affect-its-pitch-rotation
[12] F1TENTH (2023). F1TETNH Autonomous Racing Organization at the University of Pennsylvania. https://doi.org/10.1007/978-3-642-33835-9-49https://f1tenth.org/